A tailor-made crop growth model for the tomato production systems in Colombia

Modelo de crecimiento de cultivo diseñado a medida para los sistemas de cultivo de tomate de Colombia

Rodrigo Gil[1], Carlos Ricardo Bojacá[1]*, and Eddie Schrevens[2]

ABSTRACT

Potential crop models simulate the plant growth under non-limiting biophysical conditions with no other factor than the climate to which the plants are exposed to. These models may fail to adequately represent the crop performance if they are not adapted to the local conditions. The particularities of Colombian tomato systems (greenhouse and open field) demand the recalibration of existing models to make a more realistic representation of those systems. Therefore, a locally calibrated crop model was proposed considering both production systems. To this purpose, four on-farm calibration experiments were carried out, two under greenhouse conditions with average temperatures of 17.4 and 17.9°C in Santa Sofía (Boyacá) and two under open field conditions in Páramo and San Gil (Santander), with average temperatures of 20.6 and 24.0°C, respectively. The crops were commercially managed according to the local practices. Plant data was collected through destructive measurements carried out on a fortnightly basis, while climate data were collected for the entire crop growth cycle. Independent calibration of the dry matter fractions allocated at the plant organs in function of thermal time resulted in an acceptable model performance. The calibration of the model under commercial conditions gave a better representation of the local systems but at the expense of accuracy since on-farm experiments cannot be controlled as those performed in research facilities.

Key words: crop modeling; cropping system; protected cultivation; thermal time; yield potential

RESUMEN

Los modelos de cultivo potenciales simulan el crecimiento de la planta bajo condiciones biofísicas no limitantes, sin más que el clima al que están expuestas las plantas. Estos modelos pueden no representar adecuadamente el rendimiento del cultivo si no se adaptan a las condiciones locales. Las particularidades de los sistemas colombianos de tomate (invernadero y campo abierto) demandan la recalibración de modelos existentes para hacer una representación más realista de esos sistemas. Por lo tanto, en el presente trabajo se propone un modelo de cultivo calibrado localmente considerando ambos sistemas de producción. Para ello, se realizaron cuatro experimentos de calibración en finca, dos en condiciones de invernadero con temperaturas promedio de 17,4 y 17,9°C en Santa Sofía (Boyacá) y dos en campo abierto en Páramo y San Gil (Santander), con temperaturas promedio de 20,6 y 24,0°C, respectivamente. Los cultivos fueron manejados comercialmente según las prácticas locales. Los datos de las plantas se recolectaron mediante muestreos destructivos realizados cada dos semanas, mientras que los datos climáticos se recolectaron durante todo el ciclo de cultivo. La calibración independiente de las fracciones de materia seca asignadas a los órganos de las plantas en función del tiempo térmico dio como resultado un rendimiento aceptable del modelo. La calibración del modelo en condiciones comerciales dio una mejor representación de los sistemas locales, pero a expensas de la precisión, ya que los experimentos en las fincas no pueden ser controlados como los realizados en instalaciones de investigación.

Palabras clave: modelado de cultivos; sistema de cultivo; cultivo protegido; tiempo térmico; rendimiento potencial

Introduction

During the last 40 years, crop systems simulation has evolved from a neophyte science with inadequate computer power into a robust and increasingly accepted science supported by improved software and computing capabilities (Boote *et al*., 2012). Over the last decade, the most significant demand of cropping system models has aimed to assess climate change impact on agriculture and to evaluate mitigation and adaptation strategies, conducted over different spatial scales and degrees of agricultural systems complexity (Stöckle *et al*., 2014).

Received for publication: 12 June, 2017. Accepted for publication: 31 October, 2017 Doi: 10.15446/agron.colomb.v35n3.65615

[1] Departamento de Ciencias Básicas y Modelado, Facultad de Ciencias Naturales e Ingeniería, Universidad Jorge Tadeo Lozano, Bogota (Colombia).
[2] Department of Biosystems, Faculty of Bioscience Engineering, University of Leuven, Leuven (Belgium).
* Corresponding author: carlos.bojaca@utadeo.edu.co

Most crop system models have evolved as elaborations of crop components and soil models focusing on modeling a single point in space over time to explore the of crop responses to soil, management and weather variability (Jones, *et al*., 2016). Regarding the crop modeling component, they simulate phenology and partitioning, and integrate processes of C, N and water balance from planting to maturity, showing the final yield and production as well as the daily values of crop components over the time to maturity (Boote *et al*., 2013). This potential yield is related to an adapted cultivar mainly determined by solar radiation, temperature, carbon dioxide, and genetic traits that lead the length of the growing period, light interception by the crop canopy and its conversion to biomass, and the biomass partition to the harvestable organs (Grassini *et al*., 2015). Under this approach, crop growth is not constrained by factors such as water, nutrients or pests.

While in the developed world the description and testing of single crop models have lost relevance (Stöckle *et al*., 2014), the development of crop growth models remains as a distant study subject to less developed agricultural productive areas. Di Paola *et al.* (2015) showed an overview of the crop growth and yield models through the unbalanced situation in which most of the available models have been applied for temperate regions and some references exhibiting examples from Brazil and Mexico. Moreover, the development of such models has been oriented towards staple crops such as cereals, sugar beet and potato.

Tomato is among the most important horticultural crops worldwide. A variety of tomato growth models have been developed in the past (i.e. Soto *et al*., 2014; Valdés-Gómez *et al*., 2014; Heuvelink, 1999; Scholberg, *et al*., 1997; Jones *et al*., 1991) with different levels of complexity and for different purposes. Tomato crop growth models have been included in decision support systems such as the world-renowned DSSAT (Jones *et al*., 2003) as well as many others (Massa *et al*., 2013; Jizhang *et al*., 2006). Moreover, 3D models of tomato plants have been developed for purposes such as optimizing LED lighting to increase light absorption and crop growth (de Visser *et al*., 2014).

In Colombia, Cooman (2002) evaluated the feasibility of a protected tomato cropping in the high altitude tropics by locally calibrating the second version of the Tomgro model through controlled experiments in the Bogota plateau. He modified the model by reducing the leaf expansion rate at low temperature and incorporating a direct effect of temperature on the distribution of dry matter between vegetative and generative plant organs. This modified version of the Tomgro model was later applied by Bojacá *et al*. (2009) to evaluate the variability of greenhouse tomato yield caused by spatial temperature variations.

However, most of Colombian tomatoes are grown throughout the year in several Andean mountain valleys and hills in warmer climates at altitudes below those of the Bogota plateau. Regarding the production context, tomato is a small-scale business represented by clusters of growers cultivating tomato by one of the two established systems: open field or greenhouse production. Under both systems, growers apply suboptimal practices despite the differences on the demand for resources per unit area (Bojacá *et al*., 2013; 2014).

As process based, crop models closely reflect the behavior of particular crops, the features of Colombian tomato systems demand the development of a locally calibrated growth model. However, this calibration is a highly data-demanding task as well as specific for the available data constraining a broader applicability (Robertson *et al*., 2013). On the other hand, most calibration experiments are carried out under controlled conditions, which in some cases are not representative of those observed under the natural field conditions (Craufurd *et al*., 2013).

Thus, the objective of the present work is to propose a simple crop growth tomato model with the ability to simulate different growth habits (open field or greenhouse) calibrated through on-farm trials, which reproduce the growing patterns and management practices applied by local farmers in Colombia. While on-farm calibration entails a series of experimental challenges, it allows the development of a more realistic model reproducing the production management practices applied by growers in the considered zones.

Materials and methods

Model description

The model structure, as presented in Figure 1, is based on earlier crop growth and transpiration models (Gil *et al*., 2017; Cooman, 2002). The model runs on a daily basis, exception made for the gross photosynthesis and maintenance respiration routines, which run on an hourly basis. All model calculations are done on a per plant basis. At the beginning of the simulation, once the climate (air temperature, relative humidity and global radiation) for the corresponding day is updated, the total dry matter production is simulated followed by its distribution among the above-ground plant organs.

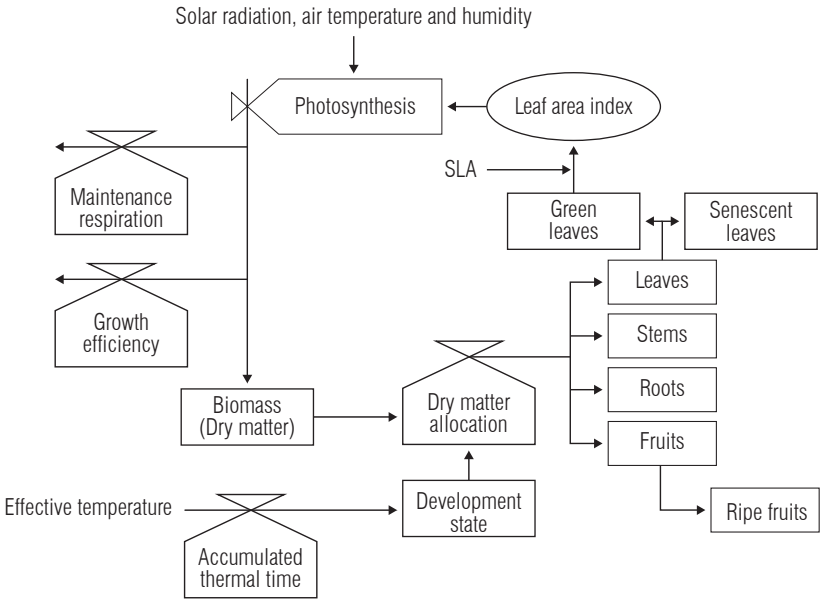

FIGURE 1. Schematics of the proposed tomato crop growth model for the open field and greenhouse production systems.

Dry matter production

The amount of dry matter available for growth is calculated at the end of the day as the difference between gross photosynthesis and total respiration. The daily gross photosynthesis results from the integration of the photosynthetic rates calculated on an hourly basis. The photosynthetic rate depends mainly on the photosynthetic active radiation (*PAR*) absorbed by the canopy, the air temperature and the CO_2 concentration, as modeled by Acock *et al.* (1978). The model considers restrictions on the photosynthetic rate due to extreme temperatures and vapor pressure deficit. These processes were modeled with the following equations:

$$GP_h = \frac{P_{MAX}}{XK} \times ln\left(\frac{(1-XM)+QE\times XK\times PPFD}{(1-XM)+QE\times XK\times PPFD\times e^{-XK\times LAI}}\right) \quad (1)$$

$$PPFD = (SolRad\times 0.47)\times 4.57 \quad (2)$$

$$P_{MAX} = \tau \times CO_2 \times PVPD \times PGRED \quad (3)$$

$$PVPD = e^{(CK\times(VPD-VPDL))} \quad (4)$$

$$PGRED = \begin{cases} 0, & if\ TMP < 9ºC \\ TMP - 9, & if\ 9 \le TMP < 10ºC \\ 1, & if\ 10 \le TMP < 28º \\ -0.083\times TMP + 3.33, & if\ 28 \le TMP < 40º \\ 0, & if\ TMP \ge 40ºC \end{cases} \quad (5)$$

Where GP_h is the hourly gross photosynthesis (g CH_2O h^{-1}), P_{MAX} is the maximum leaf photosynthetic rate (µmol CO_2 m^{-2} s^{-1}), *XK* is the light extinction coefficient, *XM* is the leaf light transmission coefficient, *QE* is the leaf quantum efficiency (µmol CO_2 μmol^{-1} photon), *PPFD* is the photosynthetic photon flux density (µmol m^{-2} s^{-1}), *LAI* is the leaf area index, *SolRad* is the hourly solar radiation (MJ m^{-2}), τ is the CO_2 use efficiency (µmol CO_2 m^{-2} s^{-1} ppm^{-1}), CO_2 is the carbon dioxide concentration in air (ppm), *PVPD* is a function that correct the P_{MAX} for air vapor pressure deficit, *CK* is a factor used to determine the effect of vapor pressure deficit on photosynthesis (kPa^{-1}), *VPD* is the air vapor pressure deficit (kPa), *VPDL* is a factor used to determine the effect of vapor pressure deficit on photosynthesis (kPa), *PGRED* is a function that correct the P_{MAX} for sub optimal temperatures and *TMP* is the hourly mean temperature (ºC).

At the end of each day hourly gross photosynthesis is integrated, and the results is transformed into the amount of carbohydrates synthesized by the plant at the current day, following this formula:

$$GP_d = \sum_{h=1}^{24}(GP_h\times 3600)\times\frac{30\times 10^{-6}}{PLM2} \quad (6)$$

where GP_d is daily gross photosynthesis (g CH_2O d^{-1}), GP_h is hourly gross photosynthesis (g CH_2O h^{-1}) and *PLM2* is the plant density (plants/m^2).

The total respiration is represented by the maintenance respiration and the growth efficiency. Daily maintenance respiration is calculated as a fraction of the accumulated dry matter in stems, active leaves and growing fruits at a reference temperature of 20ºC. Afterwards, the maintenance respiration is corrected for temperature using a Q_{10} value. Next we present the equations that describe this module.

$$M_{RES} = Q_{10}^{0.1(TM\times P-2.0)}\times(\text{RMRL}\times(DMl + DMs) + RMRF \times DMf) \quad (7)$$

where M_{RES} is the maintenance respiration per day (g CH_2O d^{-1}), TMP_{avg} is the daily average temperature (°C), *RMRL* is a respiration coefficient for stem and leaves tissues (g CH_2O g^{-1} DM d^{-1}), *DMl* is the dry matter in leaves (g DM), *DMs* is the dry matter in stems (g DM), *RMRF* is a respiration coefficient for growing fruits (g CH_2O g^{-1} DM d^{-1}) and *DMf* is the dry matter in fruits (g DM).

Based on the above, the daily biomass production per plant is calculated using the following expression:

$$DMp = (GP_d - M_{RES})\times GREF \quad (8)$$

Where *DMp* is the total dry matter produced at day (g DM d^{-1}), GP_d is the daily gross photosynthesis (g CH_2O d^{-1}), M_{RES} is the maintenance respiration per day (g CH_2O d^{-1}) and *GREF* is a growth efficiency coefficient (g DM g^{-1} CH_2O).

Dry matter distribution

We considered the organs in the model as single units (i.e. big leaf model approach), meaning no dry matter distribution occurred among cohorts or sympodial units. The dry matter fabricated each day is allocated to the plant organs through thermal time (*TT*, °Cd) dependent functions. Each function describes the proportion (on a scale from 0 to 1) of the daily dry matter assigned to the considered organ. The base temperature at which plant growth starts was set at 10°C (Valdés-Gómez *et al.*, 2014). A fixed fraction (9%) of the dry matter produced was allocated to the roots. The equations describing dry matter distribution are:

$$DM_l = DMp\times\left(\frac{c_l}{1+a_l\times e^{-b_l\times ATT}} + d_l\right) \quad (9)$$

$$DM_f = DMp\times\left(\frac{c_f}{1+a_f\times e^{-b_f\times ATT}}\right) \quad (10)$$

$$DM_s = DMp - \left(DM_l + DM_f + DM_r\right) \quad (11)$$

Where *DMp* is the total dry matter produced at day (g DM d^{-1}), DM_l is the daily dry matter allocated to leaves (g DM d^{-1}), DM_f is the daily dry matter allocated to fruits (g DM d^{-1}), DM_s is the daily dry matter allocated to stems (g DM d^{-1}), DM_r is the daily dry matter allocated to roots (g DM d^{-1}), *ATT* is accumulated thermal time (°Cd) and a_i, b_i, c_i and d_i are the parameters that must be fitted for each function, and the sub index *i* represents the corresponding plant organ (leaves and fruits).

Once leaf senescence starts, the fraction of dry matter distributed to these leaves was estimated as a function of the ATT. When the harvest begins, we applied the same approach for the ripe fruits. The daily leaf area was calculated as the total dry matter corresponding to the active leafs multiplied by the specific leaf area (SLA). The proportion of senescent leaves was calculated in the following way for open field tomatoes:

$$SEN_l = \begin{cases} 0, & if\ ATT < 677 \\ 1.08\times10^{-3}\times ATT - 0.73, & if\ 677 \le ATT \le 1600 \\ 1, & ATT > 1600 \end{cases} \quad (12)$$

While for tomatoes under greenhouse it was calculated as follows:

$$SEN_l = \frac{c_{sen}}{1+a_{sen}\times e^{-b_{sen}\times ATT}} \quad (13)$$

where SEN_l is the rate of senesces for leaves, *ATT* is accumulated thermal time (°Cd), a_{sen}, b_{sen}, and c_{sen}, are the parameters to be fitted. On the other hand, ripe fruits ready to be harvested were calculated with the following function:

$$F_{hvt} = TDM_f\times\left(\frac{c_{rf}}{1+a_{rf}\times e^{-b_{rf}\times ATT}}\right) \quad (14)$$

where F_{hvt} is the dry matter of ripe fruits (g DM), TDM_f is the accumulated dry matter in fruits throughout the crop cycle (g DM), *ATT* represents the accumulated thermal time (°Cd) and a_{rf}, b_{rf}, and c_{rf}, are the parameters that must be fitted. The leaf area (*LA*) per plant was calculated based on the *DM* allocated to leaves and the *SLA* according to the following expression:

$$LA = TDM_{gl}\times SLA \quad (15)$$

$$DM_{gl} = TDM_l\times(1 - SEN_l) \quad (16)$$

where *LA* is the plant leaf area (m^2 $plant^{-1}$), TDM_{gl} is total dry matter belonging to photosynthetically active leaves (g DM), *SLA* is the specific leaf area (m^2 g^{-1}) estimated as 0.019 and 0.021 for greenhouse and open field tomatoes, respectively, TDM_l is total dry matter allocated in leaves (g DM) and SEN_l is the rate of senesces for leaves. Finally, the *ATT* was calculated as follows:

$$ATT = \sum_{d=1}^{nd} T_{ef} \quad (17)$$

$$T_{ef} = \begin{cases} 0, & if\ TMP_{avg} \le T_b \\ TMP_{avg} - T_b, & if\ TMP_{avg} > T_b \end{cases} \quad (18)$$

where *ATT* is accumulated thermal time (°Cd), *nd* is the number of days of the growing cycle, T_{ef} is the daily effective temperature (°C), TMP_{avg} is the daily average temperature (°C) and T_b is the base temperature (10°C). The values of the parameters included in the previous models equations are shown in Tab. 1; while the values of the fitted parameters values (a_i, b_i, c_i, d_i) for the equations 9, 10, 13 and 14 are shown in the Results section.

TABLE 1. Parameters included in the tomato growth model.

Meaning	Abbreviation	Value	Units
Air carbon dioxide concentration	CO_2	360	ppm
Light extinction coefficient	*XK*	0.58	Dimensionless
Leaf light transmission coefficient	*XM*	0.091	Dimensionless
Leaf quantum efficiency	*QE*	0.0645	μmol CO_2 μmol^{-1} photon
Carbon dioxide use efficiency	τ	0.0693	μmol CO_2 m^{-2} s^{-1} ppm^{-1}
Sensitivity to temperature	Q_{10}	1.4	Dimensionless
Effect of VPD on photosynthesis	*VPDL*	4.0	kPa
Effect of VPD on photosynthesis	*CK*	-0.8	kPa^{-1}
Respiration rate for leaves and stems	*RMRL*	0.015	g CH_2O g^{-1} DM d^{-1}
Respiration rate for fruit	*RMRF*	0.01	g CH_2O g^{-1} DM d^{-1}
Overall conversion efficiency	*GREF*	0.75	g DM g^{-1} CH_2O

Crop model calibration

Field experiments

The experimental work was conducted during 2016 in four commercial tomato production plots, with two of them planted under open field and the other two under greenhouse conditions. On each case, the crops were planted and managed according to the commercial practices regularly applied by growers under each production system. The crops were planted in two of the most representative tomato production areas of Colombia. The Alto Ricaurte province, located in the department of Boyaca, is one of the major greenhouse tomato production areas in Colombia, while the Guanenta province situated in the department of Santander is an important production area for open field vegetables including tomato. Tab. 2 describes the general characteristics of the experiments carried out to calibrate the proposed crop growth model. Next, we present a general description of the management practices applied in the experimental fields for both production systems.

The protected experiments were carried out under plastic naturally ventilated greenhouses with wooden structure. Plants were grown on a single stem of indeterminate length by periodically removing side shoots. Plants were tutored following the high wire system and no fruit pruning was done whatsoever. After harvest began, the leaves located under the harvested truss were removed since these no longer contributed to the plant growth and were more susceptible to be infected by fungal diseases. Nutrients were delivered through a fertigation system along with the irrigation water.

For the open field experiments, determinate growth cultivars grew freely without doing any leaf or fruit pruning, hanging the shoots to an elevated wire. Solid fertilization was done throughout the cropping cycle with amounts and timing defined by each grower. Fertilization for each location was based on soil analysis results, and the nutrients demanded by the plant to achieve potential yields. Under greenhouse, the fertilization of macronutrients was defined based on the following reference extractions: 10, 6.7 and 20 g/plant for nitrogen (as total nitrogen), phosphorus (as P_2O_5) and potassium (as K_2O), respectively. For the open field plots, the reference values were 12.3, 6.9 and 19.3 g/plant of nitrogen (as total nitrogen), phosphorus (as P_2O_5) and potassium (as K_2O), respectively. These values were obtained from the literature (Besford and Maw, 1974; Hernández *et al*., 2009; Atherton and Rudich, 2012) and adjusted based on previous trials conducted. The fertilization was divided into two periods taking into account the plant development stage. The establishment stage was defined from the sowing until the appearance of the first truss while the second one corresponded to the fruits development.

We took into account that the first stage has a shorter duration and that during most of the tomato cycle, the plants alternate between vegetative and generative growth. The fertilization fragmentation was done as follows: 30% of nitrogen and phosphorus, and 20% of potassium during the establishment and the rest during the fruit development stage. In the open field, the fertilizers used were ammonium nitrate, diammonium phosphate and potassium chloride, while under greenhouse the sources were calcium nitrate, monoammonium phosphate, and potassium sulfate. In the open field plots, we applied the fertilizers manually on a fortnightly basis, while under greenhouse we did it through the fertigation system three times a week. Under both systems, pest management was entirely based on chemically synthetized pesticides and with a spraying schedule defined according to the grower's criteria.

Data collection

The model calibration data were collected through a series of destructive measurements carried out for each experimental plot. Starting at transplanting time and on

TABLE 2. General characteristics of the on-farm experiments used to calibrate the tomato crop growth model.

Plot code	Production system	Location	Altitude (m a.s.l)	Planting date	Cycle length (days)	Density (plants/m^2)	Cultivar	Plot area (ha)
GH1	Greenhouse	5º 42' 26.7'' N – 73º 36' 4.1'' W	2346	28/01/2016	131	3.0	Libertador	0.28
GH2	Greenhouse	5º 44' 8.0'' N – 73º 36' 13.1'' W	2347	28/03/2016	113	3.9	Roble F1	0.28
OF1	Open field	6º 25' 15.4'' N – 73º 11' 56.7'' W	1703	27/01/2016	82	1.3	DRD	4.0
OF2	Open field	6º 28' 55.4'' N – 73º 6' 54.7'' W	1140	27/01/2016	97	1.3	Roble F1	1.0

a fortnightly basis, the aerial part of three plants from each experimental plot was removed. Under all conditions, the sampled plants were surrounded by edge plants. Afterwards, the plants were divided into its organs and weighted after being oven dried at 70ºC for at least 72 h. The leaf weight included the weight of the blades and all petioles.

Once fruit harvest and leaf pruning began, the amount of biomass removed from the plant was registered, and a sample was taken to determine its dry matter content. The grower defined the frequency and amount of biomass harvested or removed according to his criteria. the leaf area was determined by taking digital pictures of all the active leaves present at the moment of the destructive measurement. From the digital pictures, the number of pixels representing the leaves was extracted, including a reference object of a known area. To discriminate the image pixels as leaves, a reference object included into a prediction tree algorithm was used. All pictures were taken at the same height through a fixed mount tripod. The corresponding leaf area was estimated through the relation between the number of pixels of the reference object and the number of pixels corresponding to the leaf surface. This image processing step was carried out with the R statistical software (R Core Team, 2015). All the data collected from fruit harvest, leaf pruning and leaf area was later then integrated on a per plant basis.

The length of the data collection calibration was a function of the grower's decision to continue with his crop. Therefore, the number of destructive measurements was variable particularly to each experimental plot. Regularly, greenhouse growers are able to extend the cropping cycle for a longer period than those of the open field system. For the greenhouse plots we were able to carry out ten and nine destructive measurements for *GH1* and *GH2*, respectively, while for the open field plots seven and eight destructive measurements for *OF1* and *OF2* were respectively performed. In all cases, the destructive measurements were carried out until the end of the cropping cycle, ensuring that the complete plant cycle was characterized through these measurements. Tab. 1 includes the duration of the crop cycle for each experiment.

As global radiation, air temperature, relative humidity and wind speed are input variables for the model, Data was collected by placing the required sensors within the experimental plots. The hourly weather was recorded using a Vantage Pro2 Weather System (Davis Instruments, Hayward, CA, USA) for each of the open field experimental plots. For the greenhouse plots, Two copper-constantan thermocouples were installed and linked to a datalogger (Cox-Tracer Junior, Escort DLS, Edison, NJ, USA) to register dry and wet bulb temperatures. Through the psychrometric relationship between these two temperatures the air relative humidity was derived. Thermocouples were placed inside a ventilated white capsule to avoid altered readings due to the sun direct radiation. The global radiation within the greenhouses was measured throughout the measurement period with a pyranometer (Model LI200RX, Campbell Scientific, Inc., Logan, UT, USA) placed at 2.5 m above the ground. A weather station was deployed (Model Vantage Pro2, Davis Instruments, Hayward, CA, USA) outside the greenhouses, registering the external hourly climate.

Dry matter partitioning calibration

The calibration of the proposed model was focused on the dry matter partitioning among organs while it is considered as a key process to define the overall growth and development of the plant. For this purpose, on each tomato system, individual models to the fractions were fitted defining the amount of daily dry matter allocated at the leaves (Equation 9) and fruits (Equation 10) as a function of *TT*. The parameters for each model were estimated through the Nelder-Mead algorithm for a derivative-free optimization (Kelley, 1999) implemented in the dfoptim package (Varadhan, 2016) of the R statistical computing software (R Core Team, 2015). The same procedure was followed for the models that defined the fractions of senescent leaves (Equation 13) and ripe fruits (Equation 14).

A fixed fraction of 9% was allocated to the dry matter of the roots (Gil *et al.*, 2017). The fraction of dry matter allocated

to the stems was calculated as the remaining fraction after discounting those allocated to fruits, leaves and roots.

The statistical analysis comparing the observed field data and the simulated values included the following statistical criteria: *Bias* (g DM/plant), root mean square error (*RMSE*, g DM/plant), and model efficiency (*EF*, dimensionless). These goodness-of-fit measures are defined according to the following equations:

$$Bias = \frac{1}{N}\sum_{i=1}^{N} D_i \quad (19)$$

$$RMSE = \sqrt{\frac{1}{N}\sum_{i=1}^{N}(D_i)^2} \quad (20)$$

$$EF = \frac{\sum_{i=1}^{N}(Y_i-\hat{Y}_i)^2}{\sum_{i=1}^{N}(Y_i-\bar{Y})^2} \quad (21)$$

Where N is the total number of observations, D_i is the difference between the measured value (Y_i) and the observed one ($\hat{Y}_i$) for the ith observation. *Bias* quantifies the average difference between measured and simulated values, with the best fit indicated when the *Bias* index is closer to zero. The *RMSE* is in the same units of the original variable and is a measure commonly used to check the agreement between measured and simulated results. *EF* is the most widely used distance measure including upper and lower bounds (Wallach, 2006). A model with an *EF* equal to one indicates a perfect fit between observed and predicted values. A full description of these goodness-of-fit measures can be found in Wallach (2006).

Results and discussion

Experimental climate conditions

The climate conditions under which the calibration experiments were carried out are summarized in Tab. 3. The climate conditions for the greenhouse experiments were similar since both greenhouses were located near to each other in the same municipality. However, by being planted in different dates resulted in some climate differences, especially those related to radiation levels. The global radiation level experienced by plants of the *GH1* experiment was higher than the one observed for the *GH2* experiment.

As the open field experiments were located at a lower altitude, these plants grew at higher temperatures with averages above 20°C. The climate of the *OF2* experiment showed the highest temperature and radiation levels as compared to the other three experiments. The lower radiation levels of the other experiments are explained due to the plastic covering in the case of the greenhouse experiments and by the geographical location of the *OF1* experiment. This open field experiment was located on top of a mountain with a permanent cloud cover, observed throughout the data collection period.

TABLE 3. Daily averages of the climate variables registered during the calibration experiments carried out under greenhouse and open field conditions

Plot code	Temperature (°C)	Global radiation (W m^{-2})	Relative humidity (%)
GH1	17.4	132.4	75.5
GH2	17.9	113.3	76.4
OF1	20.6	123.9	82.6
OF2	24.0	220.3	76.9

The temperatures registered in the open field experiments were more suitable for tomato cropping than those of the greenhouse experiments. Despite the use of plastic coverings, the average temperature of the night hours (18:00-5:00) were 15.4 and 14.8°C for the *GH1* and *GH2* experiments, respectively, while for the *OF1* and *OF2* experiments were 18.5 and 21.3°C, respectively. During the day hours (6:00-17:00), the *GH1* experiment showed an average temperature of 19.4°C while the temperature within the *GH2* experiment was warmer with an average of 21°C. Higher daily temperatures were observed for the open field experiments with averages of 22.8 and 26.7°C for *OF1* and *OF2*, respectively.

Dry matter distribution calibration

The dry matter allocation to the plant organs is a process linked to the total dry matter accumulation of the plant. Since the daily amount of assimilates produced by the photosynthesis process is a function of the climate conditions but also of the available leaf area, then the dry matter fraction allocated to the leaves defines the daily dry matter produced by the plant. Therefore, with the calibration of the dry matter distributed to leaves and fruits, we simultaneously calibrated the total dry matter plant accumulation. The fitted parameters of the functions defining the fractions of daily dry matter allocated to leaves (Equation 9), fruits (Equation 10), senescent leaves (Equation 13) and ripe fruits (Equation 14) as a function of *TT* are presented in Tab. 4.

As the dry matter distribution fractions were calibrated as a function of *TT*, next we present the cumulated *TT* of the four experiments. The highest accumulation of *TT* was achieved by the *OF2* experiment with a value of 1,371.5°Cd and followed by GH1 with 972.5°Cd. *GH2* and *OF1* experiments reached similar *TT*s of 888.7 and 885.6°Cd, respectively. Since the dry matter distribution

TABLE 4. Fitted parameters for the dry matter allocation in leaves (DM_l) and fruits (DM_f), leaves senescence rate (SEN_l) and ripening fruit rate (F_{hvt}).

Fraction	Open field				Greenhouse			
	a	***b***	***c***	***d***	***a***	***b***	***c***	***d***
Dm_l	0.044	-0.005	0.547	0.251	0.006	-0.012	0.377	0.301
Dm_f	51.34	0.006	0.521	-	136.23	0.012	0.543	-
SEN_l	-	-	-	-	3,239.37	0.011	0.735	-
F_{hvt}	10,830	0.009	0.668	-	1,000.00	0.009	0.668	-

fractions are calibrated in function of temperature we remove the time effect, allowing a more general application of these temperature-dependent functions. Therefore, the temperatures under which the plants grew are determinant for their development process rather than the cycle length.

The graphical representation of the dry matter distribution functions to the plant organs is depicted in Figure 2. The initial calibration procedure considered unique dry matter distribution functions for both tomato types. However, the results of this calibration procedure and the lower values of the goodness of fit measures indicated that independent calibration procedures should be followed for each tomato production system.

As stated previously, the fraction allocated to the roots was fixed to 0.09, while for the aboveground organs, the calibration was carried out for the leaves and fruits fractions. After adding up all the fractions, the stem fraction was the one needed to reach the total amount of dry matter produced as a function of *TT*. The comparison between production systems, exhibit the differences in the dry matter allocation to the plant organs. Under greenhouse conditions, tomatoes showed a higher decline in the dry matter allocated to the leaves and stems as compared to the situation observed for the open field tomatoes. Even under open field conditions, the plant starts allocating a higher proportion of assimilates to the leaves and then, the stem fraction increases and stabilizes to a value of 0.2.

The observed behavior of the organ fractions is defined by the growing habit of each tomato type and the way each production system is handled by the growers. Under open field conditions, tomato cultivars are mostly related to a determinate growth rate and growers do not apply any shoots pruning. Therefore, these plants have a higher stem fraction as compared to the indeterminate single-stem tomatoes planted under greenhouse conditions.

After a longer vegetative growth stage, the photosynthetically active leaves fraction of the open field plants declines to a minimum at the end of the growing cycle. Most of

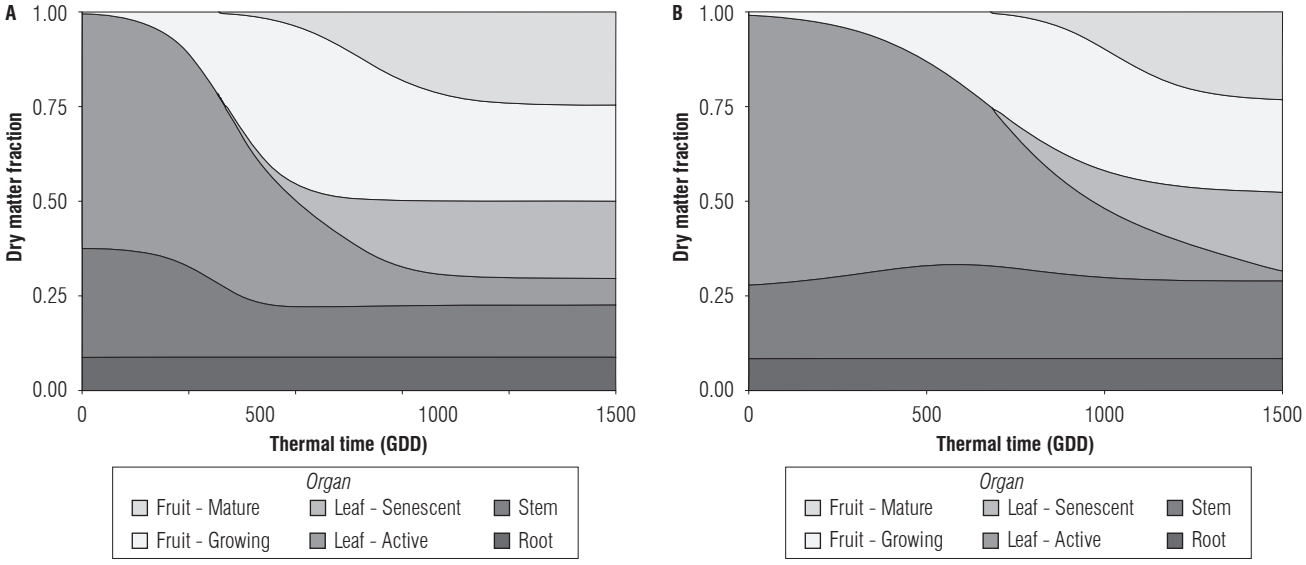

FIGURE 2. (A) Greenhouse and (B) open field tomato dry matter distribution fraction as a function of thermal time for each of the plant organs and its stages.

the remaining leaves hanging on the plant belong to the senescent fraction. On the other hand, a higher and constant fraction of active leaves is observed for the greenhouse plants, a situation that is characteristic of their indeterminate growth habit.

The fraction allocated to the fruits in the open field tomatoes showed a gentle slope as compared to the trend observed for the greenhouse conditions. However, at the end of the growth cycle, the fraction of ripe and growing fruits takes over about half of the dry matter produced by the plant. While the same pattern is observed for greenhouse tomatoes, in this case the fruits fraction is stabilized and remains constant at around the 1000°Cd. Under both production systems, it is important to note the fraction of growing fruits that remain on the plant. As the crop is reaching the end of its production cycle, the amount of harvested fruit should be higher than the one remaining in the plant, especially in the case of open field tomatoes. Nevertheless, under the local conditions growers do not properly balance the vegetative and generative growth of the plant nor apply proper pollination and pruning strategies, leading to this kind of results.

Once the dry matter distribution functions for each tomato type were calibrated, they were incorporated into the model. The observed and simulated total dry matter per plant and its allocation to the plant organs is presented in Figure 3. In most cases, the simulated dry matter properly followed the pattern depicted by the observed field data. The observed data also included not only the average of the sampled plants but also the standard deviation as a dispersion measure. Especially for the open field experiments and in particular for the last destructive measurements, there was an important variation in the data collected in the field.

Table 5 presents the goodness of fit measures selected to establish the crop growth model performance as compared to the observed field data. As the dry matter allocation fractions to the plant organs were estimated independently to each tomato type, we also present the goodness of fit measures per type of production system. According to the results for the whole plant and for each organ, a better model is considered to fit to the open field condition since values were closer to zero than the obtained ones for greenhouse tomatoes (Tab. 5). In most cases, the *Bias* results are positive indicating that the model tends to under-predict especially for the fruit dry matter since the higher *Bias* value was obtained for this organ and for both systems. The under-prediction reported by this index is a common pattern observed in particular for the first measurement dates (Fig. 3). Only the *Bias* for the total dry matter per plant in the open field condition was negative, indicating an overall over-prediction of the model but the *Bias* as such was close to zero (Tab. 5).

According to the results, the highest *RMSE* was obtained for the total dry matter per plant of the open field plants. The *RMSE* for the other plant organs and also for the results of the greenhouse plants yielded comparable *RMSE* values. Looking only at the results for the organs, the simulated dry matter allocated to the fruits gave the lowest fit under both production systems.

For the present case, the crop model reached similar *EF* values when considering the simulated dry matter per plant for both production systems. The lowest degree of agreement was observed for the simulated stem dry matter allocated to the greenhouse plants. For both production systems, the simulated fruit dry matter yielded a better fit than the one simulated for the leaves (Tab. 5).

Previous modeling efforts applied to Colombian greenhouse tomatoes such as the one carried out by Gil *et al.* (2017) whom yielded a *RMSE* of 4.21 g DM/plant for the simulated total plant dry matter. This potential crop growth model was calibrated based on experimental crops planted in the Bogota plateau and carried out under the best management possible practices without any technical constraints.

The calibration of the present model yielded comparable results to those obtained on other tomato models calibrations. For instance, Battista *et al*. (2015) calibrated a

TABLE 5. Goodness of fit measures of the simulated dry matter per plant and per organ by the calibrated tomato crop growth model.

Plant organ	Greenhouse system			Open field system		
	Bias **(g DM/plant)**	***RMSE*** **(g DM/plant)**	***EF***	***Bias*** **(g DM/plant)**	***RMSE*** **(g DM/plant)**	***EF***
Plant	13.77	22.68	0.97	-2.46	61.24	0.91
Stem	0.67	10.66	0.57	0.81	19.89	0.82
Leaf	10.0	14.76	0.86	3.69	25.42	0.80
Fruit	14.72	22.51	0.91	11.8	27.09	0.94

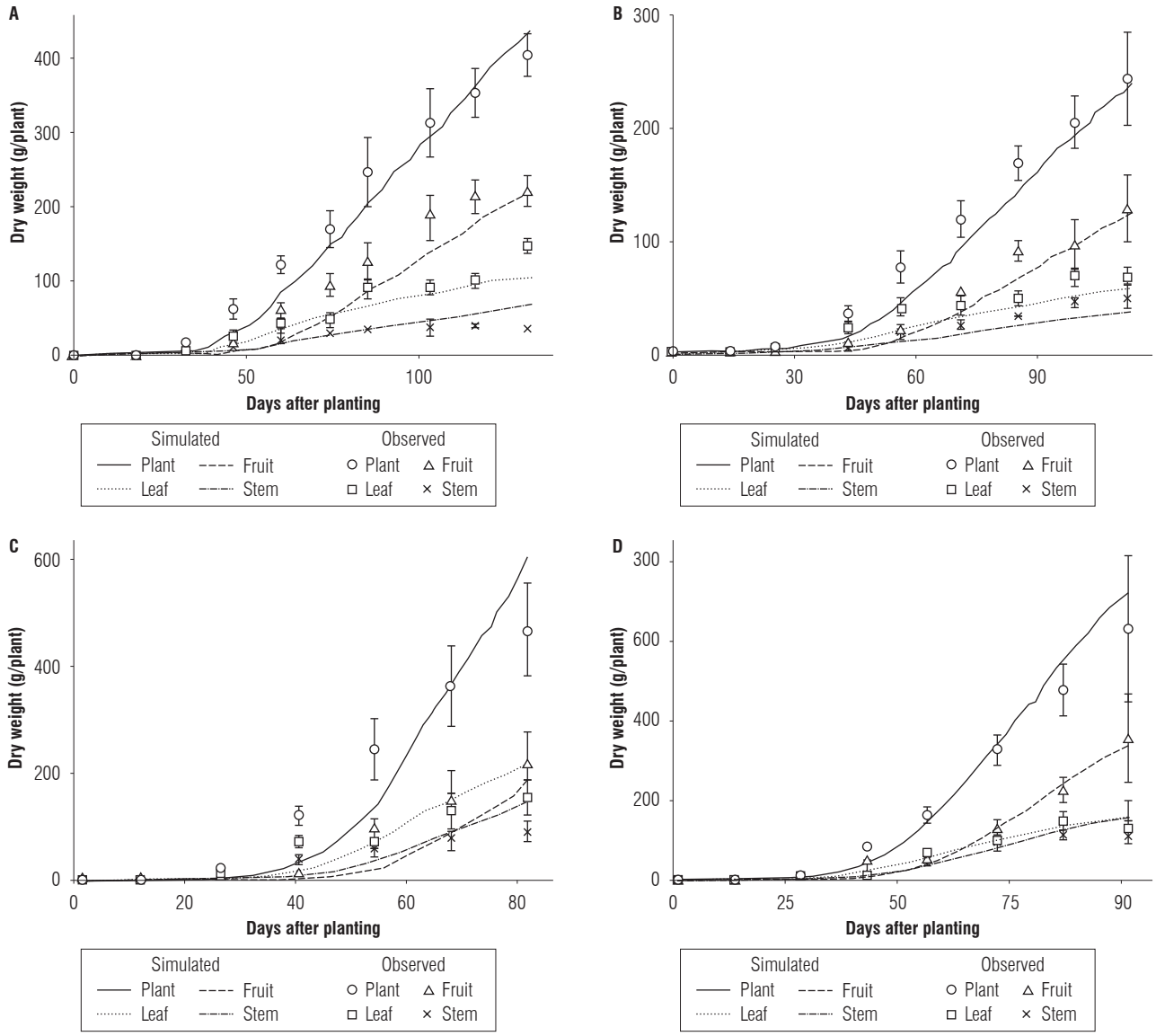

FIGURE 3. Observed and simulated dry matter accumulation and distribution over the plant organs for the calibration experiments carried out under (A, B) greenhouse and (C, D) open field conditions. Vertical bars represent the estimated standard deviation.

modified version of the Tomgro model on tomatoes growing under low-tech Italian greenhouses. The plant dry matter calibration for three cultivars indicated *RMSE* values ranging from 15.4 to 48.5 g/plant and *EF* values between 0.852 and 0.976. The paper of Fan *et al.* (2015) described a knowledge and data-driven modeling approach to simulate the growth of the tomato plant. In this case, the *RMSE* for the plant dry matter simulated with different modeling techniques ranged from 20.95 to 35.73 g/plant. The present study results are comparable to those results (exception made for the plant dry matter estimated for the open field tomatoes).

Under non-limiting growth conditions but with the biophysical constraints imposed by developing the model calibration through on-farm experiments, the proposed tomato growth model yielded acceptable results. It is important to highlight that the on-farm calibration experiments were carried out with the required rigor from the data collection point of view but were developed under the current set of management practices applied by most growers in the included zones. It is well known that on-station research results often do not reflect crop yield when technologies are applied onto surrounding farms (Leeuwis, 2004). Therefore, the model calibration was carried out through

on-farm experimentation while accounting for real world factors due to less consistent crop management.

Yield gap represents the difference between yield achieved by farmers and potential yield (Guilpart *et al.*, 2017). Different yield gaps can be established depending on the reference point used to evaluate the current yield obtained by local growers (Titonell and Giller, 2013). The first gap is obtained by comparing potential yields, with no restrictions other than those imposed by climate conditions, and those currently obtained by local farmers. Potential yields can be calculated based on models calibrated with data obtained from perfectly-controlled conditions. This gap is narrow in areas where production is characterized by high technological levels and where factors such as soil fertility and pests and diseases pressure do not impose major restrictions on the crop development. However, the current gap for both production systems is huge, and therefore impractical to establish improvement strategies, since both systems are characterized by a low technological level, which causes a high susceptibility to biotic (e.g. pest and diseases pressure) and abiotic (e.g. low soil fertility) constraints.

The second gap corresponds to the difference between the attainable yields, which correspond to the maximum yields that could be obtained given technological and environmental restrictions at a certain region and the yields currently obtained by growers. In the present work, the proposed model is calibrated using maximum achievable yield data given the local conditions; therefore, constitutes a useful tool to determine a gap that serves as a reference to design strategies that allow its reduction. Additionally, the model opens the possibility to add modules to study the factors (e.g. fertilization and irrigation strategies) that should be optimized to gradually move towards potential yields.

Another driving factor to explain the model performance is the variability introduced by the genetic factor. Mavromatis *et al.* (2001) stated that successful use of crop models in technology transfer requires coefficients describing new cultivars to be available as soon as the cultivars are marketed. On the other hand, current market trends including specialization have led to genetic differentiation in contemporary tomato varieties (Sim *et al.*, 2011). While the genetic variation is recognized, this factor was overlooked since the purpose of the proposed model is to be as generic as possible. Future improvements on the model performance can be achieved by including the genetic variation since temperature effects on crop yield are also recognized as cultivar-dependent (Vanhoor *et al.*, 2011).

Conclusions

The particularities of cropping systems, such as the case of Colombian tomatoes, demand local calibration of crop growth models. Potential growth models are far from depicting the real behavior of the crop since the conditions under which these models are calibrated are not representative of the local practices. While the tomato cultivars planted in Colombia have all the potential to achieve higher yields, these are restricted by the conditions under which the crop is managed.

The present crop growth model was developed bearing in mind this situation, therefore we calibrated it through on-farm experiments. Although the calibration of a model will never be considered complete or sufficient, the present model sets a baseline for further improvements to get a closer picture of the current tomato production systems. Contrary to our original expectations, differences in the dry matter distribution to the plant organs among greenhouse and open field tomatoes were found, therefore it was necessary to derive independent functions to characterize each tomato type. Despite including these two sets of functions, the crop model is conceived as one entity able to simulate the plant behavior for both types of tomato.

The tomato model proposed in this study is characterized by a fair compromise between representativeness and accuracy. The on-farm calibration experiments entailed a series of challenges and technical issues, commonly tackled in commercial agriculture, reducing the potential yield achievable by the crop. Consequently, by doing the calibration under these settings, the outcome model resembles more closely the reality of the current crop performance. This result comes at the expense of accuracy since higher variability is observed in the field as compared to experiments carried out in dedicated facilities and with all the resources at disposal to achieve the best possible results.

Acknowledgments

This study was funded by the Colciencias project "Desarrollo de un prototipo de sistema de soporte a la decisión para el manejo del agua y la nutrición del tomate a campo abierto y bajo invernadero" - Code: 1202-669-45624.

Literature cited

Acock, B., D.A. Charles-Edwards, D.J. Fitter, D.W. Hand, L.J. Ludwig, J.W. Wilson, and A.C. Withers. 1978. The contribution of leaves from different levels within a tomato crop to canopy net photosynthesis: An experimental examination of two canopy models. J Exp Bot. 29, 815-827. Doi: 10.1093/jxb/29.4.815

Atherton, J. and J. Rudich (eds.). 2012. The tomato crop: a scientific basis for improvement. Springer Science & Business Media Dordrecht, The Netherlands.

Battista, P., B. Rapi, A. Raschi, M. Romani, D. Massa, G. Carmassi, C. Diara, L. Incrocci, and A. Pardossi. 2015. Modified TOMGRO outputs as guide factors to estimate evapotranspiration and water use efficiency of three tomato fresh cultivars, grown in a low-tech Italian greenhouse. Acta Hortic. 1150, 39-46. Doi: 10.17660/ActaHortic.2017.1150.6

Besford, R.T. and G.A. Maw. 1974. Uptake and distribution of potassium in tomato plants. Plant Soil, 41(3), 601-618. Doi: 10.1007/BF02185819

Bojacá, C.R., K.A.G. Wyckhuys, and E. Schrevens. 2014. Life cycle assessment of Colombian greenhouse tomato production based on farmer-level survey data. J Clean Prod. 69, 26-33. Doi: 10.1016/j.jclepro.2014.01.078

Bojacá, C.R., L.A. Arias, D.A. Ahumada, H.A. Casilimas, and E. Schrevens. 2013. Evaluation of pesticide residues in open field and greenhouse tomatoes from Colombia. Food Control 30, 400-403. Doi: 10.1016/j.foodcont.2012.08.015

Bojacá, C.R., R. Gil, and A. Cooman. 2009. Use of geostatistical and crop growth modeling to assess the variability of greenhouse tomato yield caused by spatial temperature variations. Comput Electron Agr. 65, 219-227. Doi: 10.1016/j.compag.2008.10.001

Boote, K.J., J.W. Jones, G. Hoogenboom, and J.W. White. 2012. The role of crop systems simulation in agriculture and environment. pp. 326-339. In: Papajorgji, P. and F. Pinet (eds.). New Technologies for Constructing Complex Agricultural and Environmental Systems. IGI Global, Hershey, PA, USA. Doi: 10.4018/jaeis.2010101303

Boote, K.J., J.W. Jones, J.W. White, S. Asseng, and J.I. Lizaso. 2013. Putting mechanisms into crop production models. Plant Cell Environ. 36, 1658-1672. Doi: 10.1111/pce.12119

Cooman, A. 2002. Feasibility of protected tomato cropping in the high altitude tropics using statistical and system dynamic models for plant growth and development. PhD thesis, Katholieke Universiteit Leuven, Leuven, Belgium.

Craufurd, P.Q., V. Vadez, S.V. Krishna Jagadish, P.V. Vara Prasad, and M. Zaman-Allah. 2013. Crop science experiments designed to inform crop modeling. Agr Forest Meteorol. 170, 8-18. Doi: 10.1016/j.agrformet.2011.09.003

De Viesser, P.H., G.H. Buck-Sorlin, and G. van Der Heijden. 2014. Optimizing illumination in the greenhouse using a 3D model of tomato and a ray tracer. Front Plant Sci. 5, 48. Doi: 10.3389/fpls.2014.00048

Di Paola, A., R. Valentini, and M. Santini. 2015. An overview of available crop growth and yield models for studies and assessments in agriculture. J Sci Food Agr. 96(3), 709-714. Doi: 10.1002/jsfa.7359

Fan, X., M. Kang, E. Heuvelink, P. de Reffye, and B. Hu. 2015. A knowledge-and-data-driven modeling approach for simulating plant growth: A case study on tomato growth. Ecol Modell. 312, 363-373. Doi: 10.1016/j.ecolmodel.2015.06.006

Gil, R., C.R. Bojacá, and E. Schrevens. 2017. Environmental savings in tomato production under optimal agrochemicals management: a modeling approach. Acta Hortic. 1154, 137-144. Doi: 10.17660/ActaHortic.2017.1154.18

Grassini, P., L.G.J. van Bussel, J. Van Wart, J. Wolf, L. Claessens, H. Yang, H. Boogaard, H. de Groot, M.K. van Ittersum, and K.G. Cassman. 2015. How good is good enough? Data requirements for reliable crop yield simulations and yield-gap analysis. Field Crop Res. 177, 49-63. Doi: 10.1016/j.fcr.2015.03.004

Guilpart, N., P. Grassini, V.O. Sadras, J. Timsina, and K.G. Cassman. 2017. Estimating yield gaps at the cropping system level. Field Crops Res. 206, 21-32. Doi: 10.1016/j.fcr.2017.02.008

Hernández, M.I., J.M. Salgado, M. Chailloux, V. Moreno, and M. Mojena. 2009. Relaciones nitrógeno-potasio en fertirriego para el cultivo protegido del tomate (*Solanum lycopersicum* L.) y su efecto en la acumulación de biomasa y extracción de nutrientes. Cultivos Tropicales 30(4), 71-78.

Heuvelink, E. 1999. Evaluation of a dynamic simulation model for tomato crop growth and development. Ann. Bot. 83, 413-422. Doi: 10.1006/anbo.1998.0832

Jizhang, W., L. Pingping, and M. Hanping. 2006. Decision support systems for greenhouse environment management based on crop growth and control cost. T. Chinese Soc. Agr. Eng. 9, 033.

Jones, J.W., J.M. Antle, B. Basso, K.J. Boote, R.T. Conant, I. Foster, C.J. Godfray, M. Herrero, R.E. Howitt, S. Janssen, B.A. Keating, R. Munoz-Carpena, C.H. Porter,C. Rosenzweig, and T.R. Wheeler. 2016. Toward a new generation of agricultural system data, models, and knowledge products: State of agricultural systems science. Agr. Sys. (article in press). Doi: 10.1016/j.agsy.2016.09.021

Jones, J.W., G.Hoogenboom, C.H. Porter, K.J. Boote, W.D. Batchelor, L.A. Hunt, P.W. Wilkens, U. Singh, A.J. Gijsman, and J.T. Ritchie. 2003. DSSAT Cropping System Model. Eur. J. Agron. 18:235-265. Doi: 10.1016/S1161-0301(02)00107-7

Jones, J.W., E. Dayan, H. Allen, H. Van Keulen, and H. Challa. 1991. A dynamic tomato growth and yield model (Tomgro). T ASAE 34, 663-672. Doi: 10.13031/2013.31715

Kelley, C.T. (ed.). 1999. Iterative methods for optimization. Society for Industrial and Applied Mathematics, Philadelphia, PA, USA.

Leewius, C. (ed.). 2004. Communication for rural innovation: rethinking agricultural extensión. Blackwell Publishing, Oxford, UK.

Massa, D., L. Incrocci, A. Pardossi, P. Delli Paoli, and A. Battilani. 2013. Application of a decision support system for increasing economic and environmentally sustainability of processing tomato cultivated in Mediterranean climate. Acta Hortic. 971, 51-58. Doi: 10.17660/ActaHortic.2013.971.3

Mavromatis, T., K.J. Boote, A. Irmak, D. Shinde, and G. Hoogenboom. 2001. Developing genetic coefficients for crop simulation models with data from crop performance trials. Crop Sci. 41, 40-51. Doi: 10.2135/cropsci2001.41140x

R Core Team. 2015. R: A language and environment for statistical computing. Viena, Austria. Retrieved from: http://www.R-project.org.

Robertson, R., G. Nelson, T. Thomas, and M. Rosegrant. 2013. Incorporating process-based crop simulation models into global economic analyses. Am. J. Agr. Econ. 95, 228-235. Doi: 10.1093/ajae/aas034

Scholberg, J.M.S., K.J. Boote, J.W. Jones, and B.L. McNeal. 1997. Adaptation of the CROPGRO model to simulate the growth of field-grown tomato. pp. 135-151. In: Kropff, M.J.; P.S. Teng, P.K. Aggarwal, J. Bouma, B.A.M. Bouman, J.W. Jones and H.H. van Laar (eds.). Applications of system approaches at the field level. Springer, Dordrecht, The Netherlands. Doi: 10.1007/978-94-017-0754-1_9

Sim, S.-C., M.D. Robbins, A. Van Deynz, A.P. Michel, and D.M. Francis. Population structure and genetic differentiation associated with breeding history and selection in tomato (*Solanum lycopersicum* L.). Heredity 106, 927-935. Doi: 10.1038/hdy.2010.139

Soto, F., M. Gallardo, C. Giménez, T. Peña-Fleitas, and R.B. Thompson. 2014. Simulation of tomato growth, water and N dynamics using the EU-Rotate_N model in Mediterranean greenhouses with drip irrigation and fertigation. Agr. Water Manage. 132, 46-59. Doi: 10.1016/j.agwat.2013.10.002

Stöckle, C.O., A.R. Kemanian, R.L. Nelson, J.C. Adam, R. Sommer, and B. Carlson. 2014. CropSyst model evolution: From field to regional to global scales and from research to decision support systems. Environ. Modell Softw. 62, 361-369. Doi: 10.1016/j.envsoft.2014.09.006

Tittonell, P. and K.E. Giller. 2013. When yield gaps are poverty traps: The paradigm of ecological intensification in African smallholder agriculture. Field Crops Res. 143, 76-90. Doi: 10.1016/j.fcr.2012.10.007

Valdés-Gómez, H., C. Gary, N. Brisson, and F. Matus. 2014. Modelling indeterminate development, dry matter partitioning and the effect of nitrogen supply in tomato with the generic STICS crop-soil model. Sci. Hortic. 175, 44-56. Doi: 10.1016/j.scienta.2014.05.030

Vanthhor, B.H.E., P.H.B. de Visser, C. Stanghellini, and E.J. van Henten. 2011. A methodology for model-based greenhouse design: Part 2, description and validation of a tomato yield model. Biosyst Eng. 111(4), 350-368. Doi: 10.1016/j.biosystemseng.2012.01.005

Varadhan, R. and H.W. Borchers. 2016. dfoptim: Derivative-free optimization. R package version 2016.7-1. Retrieved from: http://CRAN.R-project.org/package=dfoptim

Wallach, D. 2006. Evaluating crop models. pp. 11-53. In: Wallach, D., D. Makowski, and J.W. Jones (eds.). Working with dynamic crop models. Elsevier, Amsterdam, The Netherlands.